THE JOURNAL OF PHYSICAL CHEMISTRY B
A JOURNAL OF THE AMERICAN CHEMICAL SOCIETY

pubs.acs.org/JPCB

Article

Enhancing Alkyne-Based Raman Tags with a Sulfur Linker

Published as part of The Journal of Physical Chemistry virtual special issue "Xiaoliang Sunney Xie Festschrift".

Yong Li,[†] Katherine M. Townsend,[†] Robert S. Dorn, Jennifer A. Prescher, and Eric O. Potma*

Cite This: *J. Phys. Chem. B* 2023, 127, 1976−1982

Read Online

ACCESS | Metrics & More | Article Recommendations | Supporting Information

ABSTRACT: Alkyne-based Raman tags have proven their utility for biological imaging. Although the alkynyl stretching mode is a relatively strong Raman scatterer, the detection sensitivity of alkyne-tagged compounds is ultimately limited by the magnitude of the probe's Raman response. In order to improve the performance of alkyne-based Raman probes, we have designed several tags that benefit from $\pi-\pi$ conjugation as well as from additional n$-\pi$ conjugation with a sulfur linker. We show that the sulfur linker provides additional enhancement and line width narrowing, offering a simple yet effective strategy for improving alkyne-based Raman tags. We validate the utility of various sulfur-linked alkyne tags for cellular imaging through stimulated Raman scattering microscopy.

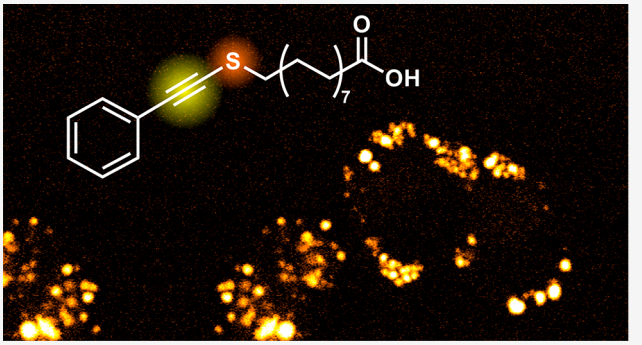

INTRODUCTION

Microscopic imaging with vibrational contrast derived from Raman spectroscopic signatures has proven itself as a label-free microscopy approach with important applications in cellular imaging. However, since the Raman spectral features of biological cells originate from the vibrational modes of common chemical motifs of bio-organic compounds, vibrational lines of a given molecular target inevitably show considerable overlap with the composite spectrum produced by all other molecular constituents in the cell. Against this background spectrum, identifying a particular biomolecular compound of interest can be challenging. This complication also limits the ability of Raman imaging to track the participation of a molecular target of interest in a given metabolic pathway.

An attractive route to overcome this limitation is to tag the molecule of interest with a small chemical motif, which exhibits a strong Raman response, yet shows a minimum spectral overlap with the Raman spectral background of the cell. Among the different chemical motifs used for Raman tagging, the alkyne moiety has been particularly successful. First introduced in 2011 as a Raman tag,[1] the strong alkyne stretching vibration is found at a frequency in the 2000−2400 cm^{-1} range where the cellular background spectrum is minimal.[1] In addition, the alkyne unit is small and shows essentially no biological activity, classifying it as a bioorthogonal probe.[2,3] The alkyne tag and its derivatives have been used extensively for linear and nonlinear Raman imaging of small molecules such as nucleic acids,[1,4−6] amino acids,[4,5] glucose,[7] fatty acids,[5−9] and more, in cells and tissues.

Although the alkyne stretching mode has a relatively high Raman cross-section, the detection sensitivity, i.e., the lowest concentration at which the tagged compound can be registered, is ultimately limited by the magnitude of the mode's Raman response. In order to improve the detection sensitivity, alternative alkyne-based motifs have been introduced that feature higher effective cross-sections. It is well-known that the Raman signal of alkynyl stretching modes can be enhanced through $\pi-\pi$ conjugation.[10,11] This can be achieved by coupling the alkyne unit to a conjugated system of sp^2-hybridized carbon such as an aromatic ring, or by conjugating it with a system of sp-hybridized carbon, or a combination of both. For instance, diyne tags and polyyne tags, which exhibit alternating triple/single carbon−carbon bonds, have enabled Raman imaging with higher sensitivity relative to a single alkyne group.[10,12,13] However, a trade-off exists between the strength of the Raman response and the size of the chemical motif, as well as its influence on the metabolic activity of the biomolecular target.

From a spectroscopic point of view, a good Raman tag exhibits an isolated vibrational band of high amplitude as well as a narrow line width. Narrow vibrational lines minimize overlap between adjacent spectral features and facilitate spectral multiplexing. Reducing the line width of a Raman

Received: December 30, 2022
Revised: February 13, 2023
Published: February 23, 2023

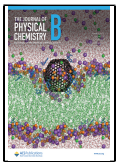

https://doi.org/10.1021/acs.jpcb.2c09093
J. Phys. Chem. B 2023, 127, 1976−1982

active mode also steepens the band shape and consequently increases its observed peak height. In principle, a narrower line width can be achieved by reducing the coupling of the vibration to other intramolecular modes, thus suppressing possible energy relaxation channels. Recent infrared absorption studies have shown that insulating the alkyne group from the molecular target with a sulfur atom can extend the vibrational coherence time, thereby compressing the spectral line width of the alkyne stretching mode.[14,15] However, Raman tag design efforts have so far paid little attention to line shape engineering.

In this work, we seek to implement the design principles of $\pi-\pi$ conjugation and line shape engineering for improving the Raman response of the alkyne tag. Using density functional theory (DFT) simulations, we first explore the Raman response of the alkyne group when attached to different chemical motifs that enable conjugation with the carbon−carbon triple bond while also insulating the tag from the target molecule through a sulfur linker. After selecting the DFT-informed designs for maximum polarizability, we synthesize and experimentally characterize their Raman spectra and evaluate their performance as a tag for stimulated Raman scattering (SRS) imaging. We show that this optimization procedure gives rise to an 8-fold enhancement of the alkyne stretching cross-section while retaining a narrow line width. When applied as a tag to palmitic acid, we further demonstrate that the designed probes are tolerated well by cells and that they are metabolically esterified in the formation of neutral lipid.

METHODS

DFT Simulations. The DFT simulations are performed in GaussView 6.0.16 software. The simulations make use of the PBEPBE method and the tzvp basis set. In all calculations, the compound is assumed to be in the gas phase. The strength of the Raman response is expressed in terms of the Raman activity S_i of the mode i, given in units of Å^4/amu. Raman intensity spectra are expressed in arbitrary units and derived from the Raman activity as follows:[11,16]

$$I_R \propto \sum_i S_i(\nu_0 - \nu_i)^4/\nu_i$$

where ν_0 is the optical frequency of the excitation laser. An excitation wavelength of 1031 nm is assumed in the simulated spectra. The calculated Raman lines are displayed as Lorentzian line shapes with a full width at half-maximum of 8 cm^{-1}.

Cell Culturing and Handling. NIH 3T3 cells were cultured in DMEM/high-glucose media supplemented with 10% fetal bovine serum (FBS) and 1% penicillin/streptomycin. HeLa cells were cultured in DMEM (Corning) containing 10% FBS (v/v, Life Technologies), 4.5 g/L glucose, 2 mM L-glutamine, penicillin (100 U/mL), and streptomycin (100 mg/mL, Gibco). Cells were passaged using 25 mL flasks. Synthesized palmitic acid probes were added to cell media as a 10× solution in DMSO. Prior to imaging, cells were seeded on glass coverslips (18 mm diameter) sitting in 12 well plates. After adhering, the cells were fixed using 4% paraformaldehyde and stabilized on standard microscope slides. The CellTiter-Glo Luminescent Cell Viability Assay (Promega) was used to evaluate cell viability.

Raman Spectroscopy Measurements. For Raman spectroscopy measurements of the probes, a small amount of the tagged compound was deposited onto a glass coverslip in solid form. Raman spectra were collected on a Renishaw InVia Raman microscope, using a 0.75 NA dry objective lens and a 1 s signal integration time. An excitation wavelength of 532 nm was used for compounds with tags Alk, Ph-Alk, and Ph-Alk-S (Table I), whereas all other compounds were measured with a 785 nm excitation wavelength in order to reduce the fluorescence background from impurities. Spectra were averaged over 30 measurements to improve the signal-to-noise ratio. For each compound, the strength of the alkynyl stretching resonance was determined relative to the methylene symmetric stretching vibration at 2850 cm^{-1}, which was used as an internal reference.

Table I. Alkynyl Resonance Frequencies (ω_o) and Raman Activities of Various Raman Tags As Predicted by DFT Simulations and As Determined Experimentally

	ω_o (cm^{-1})		Raman activity (Å^4/amu)	Rel. Raman intensity
Tag	DFT	Exp	DFT	Exp
Alk	2162	2111	283.9	1
Ph-Alk	2262	2234	2931	1.4
Ph-Alk-S	2181	2168	4184	7.9
Pyr-Alk-S	2177	2178	4135	5.5
TP-Alk-S	2158	2157	4966	5.9
TIPS-Alk-S	2106	2097	1650	2.4
Butyl-Alk-S	2206	2186	1293	0.83

Stimulated Raman Scattering Imaging Experiments. The light source for the SRS imaging experiments was an 80 MHz, picosecond optical parametric oscillator (OPO, APE picoEmerald) synchronously pumped by the frequency-doubled output of a 2 ps, 1031 nm fiber laser (aeroPULSe, NKT photonics). The residual 1031 nm light was intensity modulated at 20 MHz and served as the Stokes beam in the SRS process. The OPO signal output was tuned in the 833−855 nm spectral range and served as the pump beam in the SRS process. The pump and Stokes beams were overlapped in time, collinearly combined on a dichroic mirror, and directed to a laser-scanning microscope (Fluoview 300 and IX71, Olympus). The beams were focused on the sample by a water immersion 1.15 NA, 40× objective lens (Olympus). The pump beam was collected in the forward direction by an oil immersion 1.4 NA condenser (Olympus), filtered by a 960 nm short pass filter, and detected by a wide-area photodiode (S3634, Hamamatsu). The photocurrent was amplified and demodulated by a lock-in amplifier (HF2LI, Zurich Instruments) at the 20 MHz reference frequency.

RESULTS

Density Functional Theory Informed Optimization of Alkyne Raman Polarizability. We first used DFT simulations to estimate the Raman response of the alkyne stretching mode for a variety of different tag designs. Although DFT simulations are unable to predict line widths, they are a good start for obtaining estimates of the Raman activity of a given mode as a function of its immediate intramolecular environment. Figure 1 shows the chemical structures of several alkyne tag designs. The basic motif is a single terminal alkyne group, which in subsequent designs is expanded at its terminus with different substituents. The predicted resonance frequencies of

https://doi.org/10.1021/acs.jpcb.2c09093
J. Phys. Chem. B 2023, 127, 1976−1982

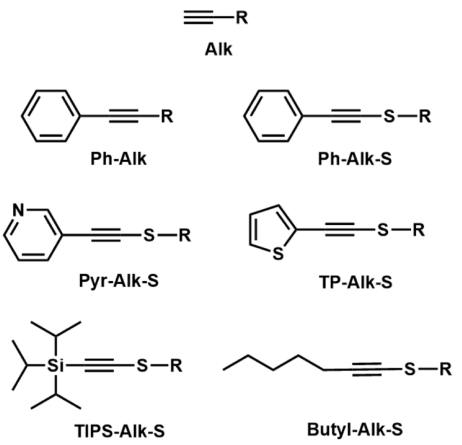

Figure 1. Alkyne-based tags studied in this work.

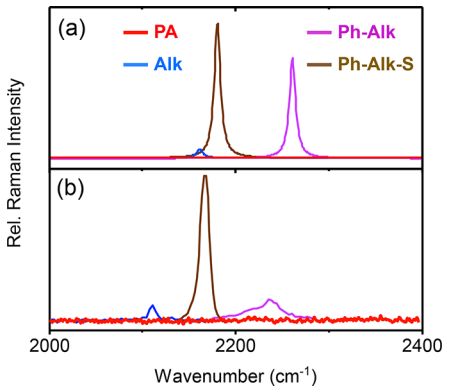

Figure 2. (a) Simulated resonance frequencies and Raman intensities of palmitic acid tagged with Alk (blue), Ph-Alk (magenta), and Ph-Alk-S (brown), as well as natural palmitic acid (red). (b) Experimental Raman spectra of the same compounds.

the alkynyl stretching modes and their corresponding Raman activities are given in Table I.

In the case of Ph-Alk, the substituent is a phenyl ring, which has already been shown to enhance the alkyne Raman activity through $\pi-\pi$ conjugation.[10] The DFT simulations confirmed the expected enhancement. As a general mechanism, the enhanced conjugation lowers the energy of the electronic $\pi-\pi^*$ transition and thus amplifies the Raman polarizability of the mode. In addition, the alkynyl vibrational resonance in the phenylacetylene motif was shifted to higher frequencies, suggesting a strengthening of the alkyne oscillator's effective spring constant.

As the main focus of this work, we examined the implication of a sulfur linkage between the alkynyl group and the target molecule, such as in compound Ph-Alk-S. The incorporation of the sulfur linker produced two effects. First, the resonance of the alkynyl stretching mode shifted to lower frequencies, indicative of a loss of rigidity of the carbon−carbon triple bond. Second, the Raman activity of the mode was increased even more. The latter effect suggests additional n$-\pi$ conjugation between the π-electrons of the alkynyl unit and the lone electron pair on the sulfur atom.[11] The DFT simulations predicted similar effects when the phenyl group was replaced by a pyridyl (Pyr-Alk-S) or thiophene (TP-Alk-S) group.

In addition, we considered an alkyne tag substituted with a triisopropylsilyl (TIPS) group to test the effect of π-backbonding of the alkynyl unit with the Si atom (TIPS-Alk-S). It is known that π-backbonding of the thio-alkyne to the Si of a substituted trimethylsilyl (TMS) group gives rise to an enhanced IR transition moment.[17] Here we examined the utility of this mechanism for enhancing the Raman response. The simulations suggest that π-backbonding with Si provides a modest enhancement of the alkynyl Raman activity, which is nonetheless less strong than that of the aromatic substituents. We also evaluated a butyl-substituted alkyne tag (Butyl-Alk-S), a probe that lacks additional π-bond conjugation via its substituent. The simulations predict that the n$-\pi$ conjugation with the sulfur linker gives rise to a stronger Raman response relative to Alk, albeit that the enhancement is less compared to that of tags with conjugation.

Enhancement of Raman Polarizability and Line Width Control. We next compared the predictions from DFT with experimental Raman spectra. Figure 2 shows the simulated and experimental Raman spectra of the basic alkyne tag and the phenylacetylene tag (Ph-Alk) and the sulfur-linked phenylacetylene (Ph-Alk-S) tag in the alkynyl stretching range. We selected palmitic acid as the molecular target. Similar to the simulations, the alkynyl stretching mode shifted to higher frequencies when the phenyl group was linked to the alkyne terminus. The observed enhancement is, however, a rather modest 1.4 times, which is less than predicted by the DFT simulations. In addition, the line width increased and the line shape appeared to reveal a shoulder on the low energy side. The appearance of a broad single line or double peaks has been reported before for different substituted phenylacetylenes and different origins of the broad spectral features have been suggested, among which is the presence of a possible Fermi resonance.[18] From the perspective of Raman tag design, line broadening is unattractive as it increases the possible spectral overlap between different tags.

In agreement with the simulation, the incorporation of the sulfur linker shifted the Raman resonance to lower frequencies. At the same time, the peak height increased and the line shape narrowed relative to the Raman signature of the phenylacetylene tag. It is possible that the additional n$-\pi$ conjugation introduced by the sulfur atom alters the resonance and steepens the line. Alternatively, the sulfur atom has been suggested to act as an insulator that effectively decouples the alkynyl stretching mode from vibrational modes in the molecular target (here palmitic acid). By limiting vibrational energy relaxation channels, the lifetime of the alkynyl stretching mode is expected to increase, resulting in a narrower line. We observed the same trend for the TP-Alk-S tag, which also showed a narrower line at lower vibrational energies compared to the same structure without the sulfur linker (see Supporting Information Figure S1).

The observation of line steepening relative to the phenylacetylene tag makes the resulting motif a good candidate for Raman imaging studies. The Ph-Alk-S tag offered an 8 times stronger Raman signal compared to the standard Alk tag without the sulfur linker. To emphasize the relative Raman response of the tag, we further compared the alkynyl stretch with the asymmetric methylene resonance of the tagged palmitic acid in Figure 3. We observed a three times stronger spectral peak for the tag compared to the total peak height of the 2880 cm^{-1} resonance of palmitic acid, underlining the brightness of the probe.

https://doi.org/10.1021/acs.jpcb.2c09093
J. Phys. Chem. B 2023, 127, 1976−1982

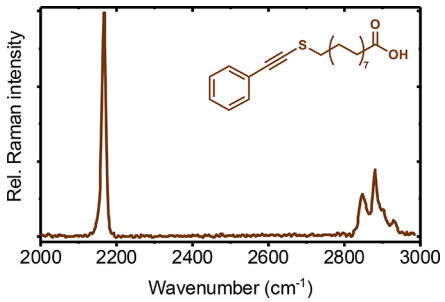

Figure 3. Raman spectrum of Ph-Alk-S-tagged palmitic acid in the 2000−3000 cm^{-1} range, comparing the intensity of the alkynyl-stretching mode with the CH-stretching modes of palmitic acid.

Figure 4 shows Raman spectra of various thio-alkyne probes, using different substituents to tune the resonance frequency of

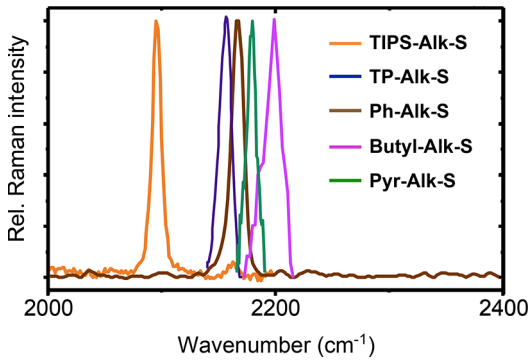

Figure 4. Normalized experimental Raman spectra of TIPS-Alk-S (orange), TP-Alk-S (blue), Ph-Alk-S (brown), Butyl-Alk-S (magenta), and Pyr-Alk-S (green).

the alkynyl stretching mode. We note that the thiophene and pyridyl substituents provide enhancement factors comparable to that of the sulfur-linked phenylacetylene tag due to $\pi-\pi$ conjugation; see Table I. The butyl-substituted thio-alkyne tag, on the other hand, lacks such conjugation and represents a much weaker Raman tag. In addition, the line-narrowing effect seen for the sulfur-linked phenylacetylene tag is absent for the alkyl-substituted thio-alkyne, indicating that the alkyl group provides an efficient pathway for vibrational energy relaxation of the alkynyl stretching mode. We note that the Pyr-Alk-S probe shows an additional strong peak at 2220 cm^{-1} in the Raman spectrum of the crystal form (not shown), which is not predicted by the simulations and which is absent when the probe is absorbed by cells. It is possible that this extra resonance originates from stacking effects in the solid phase.

We also tested experimentally whether the mechanism of π-backbonding can provide a means for enhancing the Raman activity of the alkynyl stretching mode. In line with the DFT simulations, our experiments with the triisopropylsilyl (TIPS) substituent confirmed that the Raman enhancement is present but modest (see Table I). These observations suggest that the mechanism of π-backbonding is less effective at boosting the alkynyl Raman response compared to its enhancement effect in IR absorption.

In general, we observed that the DFT simulations correctly predicted the overall trends in terms of the spectral shift of the alkynyl mode upon different substitutions. On the other hand, the experimentally observed enhancement of the tags relative to Alk was generally lower than what was predicted by the calculations.

Cellular Uptake and Esterification of Tagged Palmitic Acid. To demonstrate the practical utility of the sulfur-linked alkyne probes, we examined the uptake and esterification of tagged palmitic acid by various cell types. In Figure 5, we show

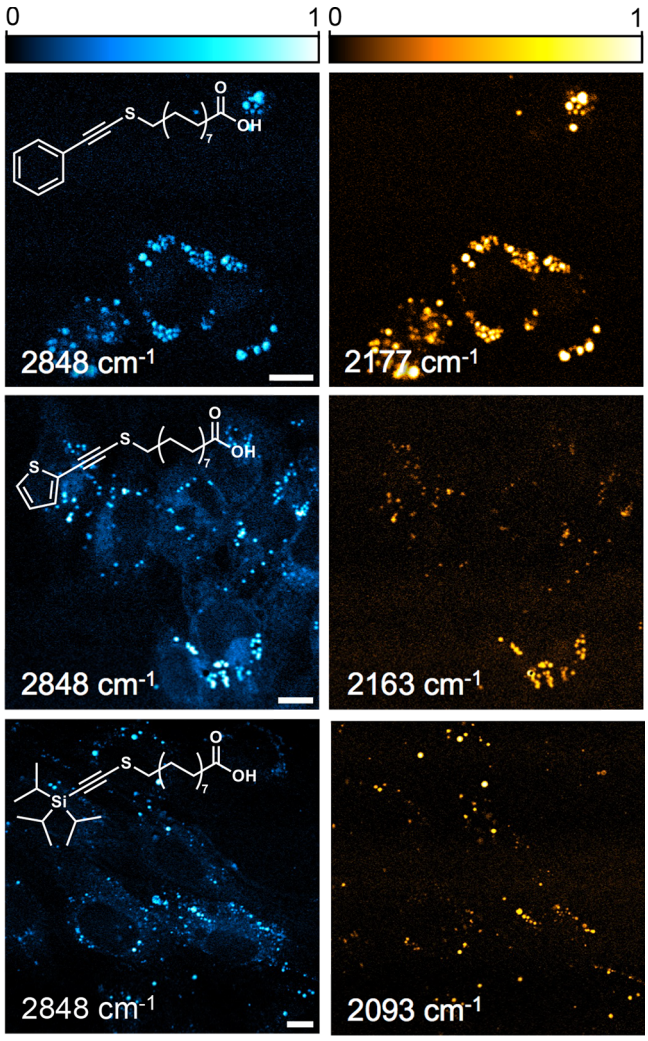

Figure 5. SRS images of NIH3T3 cells incubated with select palmitic acid probes Ph-Alk-S (top), TP-Alk-S (middle), and TIPS-Alk-S (bottom). Left column shows the SRS images taken at 2848 cm^{-1}, whereas the right column shows images taken at the maximum of the alkynyl stretching mode (bar = 10 μm).

SRS images of NIH 3T3 cells that were incubated with 25−50 μM tagged palmitic acid in the growth medium for at least 12 h. We observed that all probes were taken up by cells and that the majority of the tagged compounds ended up in lipid droplets (LDs). Lipid droplets serve as reservoirs of neutral lipids, where fatty acids are found in esterified form such as triglycerides or cholesteryl esters.[19] In particular, we found that the sulfur-linked thiophene and phenylacetylene-tagged compounds showed especially high levels of accumulation in LDs, suggesting efficient metabolic conversion of the tagged fatty acid to neutral lipid. Compared to the Ph-Alk-S and TP-Alk-S probes, we observed that the accumulation of the TIPS-Alk-S probe in LDs was generally less, indicating a somewhat

https://doi.org/10.1021/acs.jpcb.2c09093
J. Phys. Chem. B 2023, 127, 1976−1982

lower affinity of the cell for the uptake and metabolic conversion of the triisopropylsilyl-substituted alkyne tag.

Importantly, the probes were well tolerated at standard imaging doses. To examine cell viability, we incubated HeLa cells for 24 h with varying concentrations of tagged palmitic acid probes. Cell viability was then measured with a standard ATP-based assay. Figure 6 shows the results for cells treated

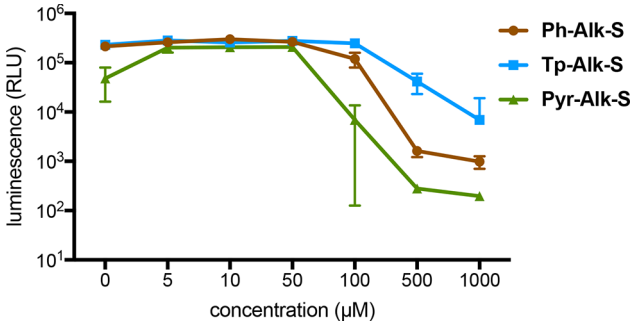

Figure 6. Viability of HeLa cells as a function of probe concentration for tagged palmitic acid. Thio-alkyne probes were incubated for 24 h (Ph-Alk-S) or for 48 h (TP-Alk-S, Pyr-Alk-S) at 37 °C.

with Ph-Alk-S, TP-Alk-S, or Pyr-Alk-S. These probes were well tolerated by cells at concentrations of 50 μM or less. Decreased cell viability was observed at higher probe doses.

A good probe traverses the same metabolic pathways as the native species. We used the sulfur-linked phenylacetylene probe for palmitic acid to test its metabolic properties. First, for low dosages of the tagged compound, we expect an increase in the amount of esterified fatty acid in the cell as its dosage in the growth medium is raised. Figure 7a shows that the ratio of the signals at the alkynyl stretching resonance over the C−H

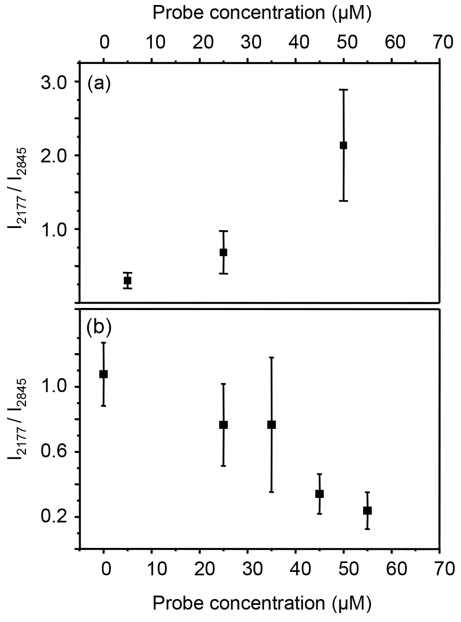

Figure 7. (a) Ratio of the SRS signal from the alkynyl stretch of Ph-Alk-S-tagged palmitic acid and the methylene stretch at 2845 cm^{-1} as a function of probe concentration in the medium. Ratio is determined at the location of lipid droplets. (b) SRS ratio as in panel a measured as a function of the concentration of natural palmitic acid in the medium while keeping the medium concentration of tagged palmitic acid at 25 μM.

stretching resonance indeed grew as the tag concentration was increased from 0 to 50 μM. This observation indicates that the tagged fatty acid is metabolically processed and stored as neutral lipid in a manner proportional to its medium concentration, as would be expected for natural palmitic acid within this concentration range. Second, if the tagged compound follows the same metabolic pathway as natural palmitic acid, we expect that the relative amount of esterified lipid observed at the alkynyl stretching frequency in a given droplet decreases as natural palmitic acid is added to the medium in increasing quantities. Figure 7b confirms that the relative concentration of tagged lipid diminished with an increasing concentration of the competing, natural palmitic acid. This result suggests that the uptake and esterification process of the tag follows the natural lipid storage pathway for palmitic acid.

DISCUSSION

In this work, we studied the Raman response of the alkynyl stretching mode as a function of its immediate intramolecular chemical environment, in an effort to further optimize the alkyne group for use as a Raman tag. Using DFT simulations, we confirmed that $\pi-\pi$ conjugation gives rise to a significant enhancement of the Raman polarizability, primarily due to the lowering of the electronic $\pi-\pi^*$ transition. The DFT results also point to the additional enhancement that can be achieved when the alkyne group is connected with a sulfur linker to the molecule of interest, a phenomenon that is attributed to n$-\pi$ conjugation with the lone electron pair on the sulfur.

Experiments confirmed the predicted enhancement. In addition, the incorporation of the sulfur linker steepens the alkynyl resonance line shape of the phenylacetylene moiety, a possible indication that the sulfur atom limits vibrational energy relaxation of the alkynyl stretching mode into the tagged molecule. This observation is in agreement with the observed narrowing of the IR line shape of the TMS-substituted alkynyl stretching mode. In that work, the sulfur atom was identified as a thermal insulator that partially decouples the tag from the rest of the molecule.[14,15] Our current work shows that a similar mechanism is likely to play a role in controlling the width of the Raman resonance. On the other hand, we have found that the mechanism of π-backbonding with a silicon atom, which has been suggested to be responsible for the enhanced IR response of the otherwise low infrared activity of the alkyne group, does not similarly improve the Raman response to the same extent. Given the symmetry of the alkyne group, it is perhaps not surprising that π-backbonding has a more dramatic effect on the IR activity of the mode compared to its effect on the corresponding Raman response.

In addition to the observed enhancement, the incorporation of a sulfur linker also gives rise to a shift in the alkyne resonance frequency. The ability to shift the resonance is relevant for multiplexed Raman imaging, in which multiple targeted compounds are differentiated through spectrally distinct Raman tags.[20] Numerous strategies for spectrally shifting alkyne-based Raman probes exist, including deuteration,[21] phenylation,[18] or silylation[22] of terminal alkynes. The use of a sulfur linker constitutes an additional strategy for spectral shifting of Raman tags probes, which can be helpful for generating expansive Raman tag libraries.

We find that most sulfur linked alkyne tags are tolerated well by cells. When linked to palmitic acid, the probes undergo the

https://doi.org/10.1021/acs.jpcb.2c09093
J. Phys. Chem. B 2023, 127, 1976−1982

expected esterification to neutral lipid after cellular uptake. The brightest probe, equipped with a sulfur-linked phenylacetylene tag, is three times as bright as palmitic acid's strongest methylene stretching resonance. In addition, our experiments show that the probe follows the same lipid storage pathway as natural palmitic acid and that the tag remains stable over a time span of days in the cellular environment (see Supporting Information Figures S2 and S3). These observations suggest that the spectroscopic advantages afforded by sulfur-linked phenylacetylene tags translate into an attractive strategy for practical Raman label studies.

CONCLUSION

Informed by DFT simulations, we have found that sulfur-linked alkyne tags offer additional advantages over existing alkyne-based Raman tags. The n−π conjugation provided by the sulfur linker combined with π−π conjugation through aromatic and heteroaromatic substituents gives rise to significant enhancement of the Raman signal from the alkynyl stretching mode. In addition, the sulfur linker reduces the line width of aromatic substituted alkyne tags, rendering them attractive for multiplex Raman labeling studies. Using tagged palmitic acid as a model system, we obtained an 8-fold signal enhancement by replacing the alkyne tag with a sulfur-linked phenylacetylene tag, while preserving cellular uptake and metabolic properties. We anticipate that enhancement of alkyne tags with a sulfur-linker offers a simple and general strategy for improving the performance of alkyne-based Raman probes, which may benefit a wide range of biological imaging studies.

ASSOCIATED CONTENT

Supporting Information

The Supporting Information is available free of charge at https://pubs.acs.org/doi/10.1021/acs.jpcb.2c09093.

Additional Raman spectra of sulfur-linked probes, off-resonance SRS images of cells, stability assays of sulfur-linked probes, general chemical information, procedure and characterization of thio-alkyne lipids, and NMR spectra of synthesized probes (PDF)

AUTHOR INFORMATION

Corresponding Author

Eric O. Potma − *Department of Chemistry, University of California, Irvine, California 92697, United States;* orcid.org/0000-0003-3916-6131; Email: epotma@uci.edu

Authors

Yong Li − *Department of Chemistry, University of California, Irvine, California 92697, United States*

Katherine M. Townsend − *Department of Chemistry, University of California, Irvine, California 92697, United States*

Robert S. Dorn − *Department of Chemistry, University of California, Irvine, California 92697, United States;* orcid.org/0000-0001-7683-2151

Jennifer A. Prescher − *Department of Chemistry, University of California, Irvine, California 92697, United States;* orcid.org/0000-0002-9250-4702

Complete contact information is available at: https://pubs.acs.org/10.1021/acs.jpcb.2c09093

Author Contributions

†Y.L. and K.M.T. contributed equally to this work

Notes

The authors declare no competing financial interest.

ACKNOWLEDGMENTS

The authors acknowledge financial support from the National Science Foundation, Grant CBET-2013814. Some of the experiments were performed with the help of the Laser Spectroscopy Laboratories, University of California, Irvine.

REFERENCES

(1) Yamakoshi, H.; Dodo, K.; Okada, M.; Ando, J.; Palonpon, A.; Fujita, K.; Kawata, S.; Sodeoka, M. Imaging of EdU, an Alkyne-Tagged Cell Proliferation Probe, by Raman Microscopy. *J. Am. Chem. Soc.* **2011**, *133* (16), 6102−6105.

(2) Scinto, S. L.; Bilodeau, D. A.; Hincapie, R.; Lee, W.; Nguyen, S. S.; Xu, M.; am Ende, C. W.; Finn, M. G.; Lang, K.; Lin, Q.; et al. Bioorthogonal chemistry. *Nat. Rev. Methods Primers* **2021**, *1* (1), 30.

(3) Wei, L.; Hu, F.; Chen, Z.; Shen, Y.; Zhang, L.; Min, W. Live-Cell Bioorthogonal Chemical Imaging: Stimulated Raman Scattering Microscopy of Vibrational Probes. *Acc. Chem. Res.* **2016**, *49* (8), 1494−1502.

(4) Hong, S.; Chen, T.; Zhu, Y.; Li, A.; Huang, Y.; Chen, X. Live-Cell Stimulated Raman Scattering Imaging of Alkyne-Tagged Biomolecules. *Angew. Chem., Int. Ed.* **2014**, *53* (23), 5827−5831.

(5) Wei, L.; Hu, F.; Shen, Y.; Chen, Z.; Yu, Y.; Lin, C.-C.; Wang, M. C.; Min, W. Live-cell imaging of alkyne-tagged small biomolecules by stimulated Raman scattering. *Nat. Methods* **2014**, *11* (4), 410−412.

(6) Chen, Z.; Paley, D. W.; Wei, L.; Weisman, A. L.; Friesner, R. A.; Nuckolls, C.; Min, W. Multicolor Live-Cell Chemical Imaging by Isotopically Edited Alkyne Vibrational Palette. *J. Am. Chem. Soc.* **2014**, *136* (22), 8027−8033.

(7) Hu, F.; Chen, Z.; Zhang, L.; Shen, Y.; Wei, L.; Min, W. Vibrational Imaging of Glucose Uptake Activity in Live Cells and Tissues by Stimulated Raman Scattering. *Angew. Chem., Int. Ed.* **2015**, *54* (34), 9821−9825.

(8) Jamieson, L. E.; Greaves, J.; McLellan, J. A.; Munro, K. R.; Tomkinson, N. C. O.; Chamberlain, L. H.; Faulds, K.; Graham, D. Tracking intracellular uptake and localisation of alkyne tagged fatty acids using Raman spectroscopy. *Spectrochimica Acta Part A: Molecular and Biomolecular Spectroscopy* **2018**, *197*, 30−36.

(9) An, X.; Majumder, A.; McNeely, J.; Yang, J.; Puri, T.; He, Z.; Liang, T.; Snyder, J. K.; Straub, J. E.; Reinhard, B. M. Interfacial hydration determines orientational and functional dimorphism of sterol-derived Raman tags in lipid-coated nanoparticles. *Proc. Natl. Acad. Sci. U. S. A.* **2021**, *118* (33), No. e2105913118.

(10) Yamakoshi, H.; Dodo, K.; Palonpon, A.; Ando, J.; Fujita, K.; Kawata, S.; Sodeoka, M. Alkyne-Tag Raman Imaging for Visualization of Mobile Small Molecules in Live Cells. *J. Am. Chem. Soc.* **2012**, *134* (51), 20681−20689.

(11) Shorygin, P. P. Raman Scattering and Conjugation. *Russ. Chem. Rev.* **1971**, *40* (4), 367.

(12) Ando, J.; Kinoshita, M.; Cui, J.; Yamakoshi, H.; Dodo, K.; Fujita, K.; Murata, M.; Sodeoka, M. Sphingomyelin distribution in lipid rafts of artificial monolayer membranes visualized by Raman microscopy. *Proc. Natl. Acad. Sci. U. S. A.* **2015**, *112* (15), 4558−4563.

(13) Lee, H. J.; Zhang, W.; Zhang, D.; Yang, Y.; Liu, B.; Barker, E. L.; Buhman, K. K.; Slipchenko, L. V.; Dai, M.; Cheng, J.-X. Assessing cholesterol storage in live cells and C. elegans by stimulated Raman scattering imaging of phenyl-diyne cholesterol. *Sci. Rep.* **2015**, *5* (1), 7930.

(14) Levin, D. E.; Schmitz, A. J.; Hines, S. M.; Hines, K. J.; Tucker, M. J.; Brewer, S. H.; Fenlon, E. E. Synthesis and evaluation of the sensitivity and vibrational lifetimes of thiocyanate and selenocyanate infrared reporters. *RSC Adv.* **2016**, *6*, 36231−36237.

(15) Ramos, S.; Scott, K. J.; Horness, R. E.; Le Sueur, A. L.; Thielges, M. C. Extended timescale 2D IR probes of proteins: p-cyanoselenophenylalanine. *Phys. Chem. Chem. Phys.* **2017**, *19*, 10081−10086.
(16) Michalska, D.; Wysokiński, R. The prediction of Raman spectra of platinum(II) anticancer drugs by density functional theory. *Chem. Phys. Lett.* **2005**, *403* (1), 211−217.
(17) Kossowska, D.; Park, K.; Park, J. Y.; Lim, C.; Kwak, K.; Cho, M. Rational Design of an Acetylenic Infrared Probe with Enhanced Dipole Strength and Increased Vibrational Lifetime. *J. Phys. Chem. B* **2019**, *123* (29), 6274−6281.
(18) Murray, M.; Cleveland, F. F. Raman Spectra of Acetylenes. I. Derivatives of Phenylacetylene, C6H5C≡ CR. *J. Am. Chem. Soc.* **1938**, *60* (11), 2664−2666.
(19) Thiele, C.; Spandl, J. Cell biology of lipid droplets. *Curr. Opin. Cell Biol.* **2008**, *20* (4), 378−385.
(20) Hu, F.; Zeng, C.; Long, R.; Miao, Y.; Wei, L.; Xu, Q.; Min, W. Supermultiplexed optical imaging and barcoding with engineered polyynes. *Nat. Methods* **2018**, *15* (3), 194−200.
(21) Bi, X.; Miao, K.; Wei, L. Alkyne-Tagged Raman Probes for Local Environmental Sensing by Hydrogen-Deuterium Exchange. *J. Am. Chem. Soc.* **2022**, *144* (19), 8504−8514.
(22) Tipping, W. J.; Wilson, L. T.; Blaseio, S. K.; Tomkinson, N. C.; Faulds, K.; Graham, D. Ratiometric sensing of fluoride ions using Raman spectroscopy. *Chem. Commun.* **2020**, *56* (92), 14463−14466.

https://doi.org/10.1021/acs.jpcb.2c09093
J. Phys. Chem. B 2023, 127, 1976−1982